Through-Wall Respiration State Detection Using Wi-Fi CSI and a Lightweight CNN–LSTM for Edge Deployment

1st Juan Ariel Mora Carrion
Faculty of Informatics and Electronics
ESPOCH
General Villamil Playas, Ecuador
juana.mora@espoch.edu.ec

2nd Diego Andres Andrade-Segarra
Faculty of Informatics and Electronics
ESPOCH
Riobamba, Ecuador
diegoa.andrade@espoch.edu.ec

3rd Deyvi Rolando Totoy Ponce
Faculty of Informatics and Electronics
ESPOCH
Guano, Ecuador
deyvi.totoy@espoch.edu.ec

***Abstract*—The growing demand for non-invasive remote healthcare has highlighted Wi-Fi Channel State Information (CSI) as a strong alternative to wearable and vision-based monitoring. This work proposes a behind-obstacle vital-signs detection system using a hybrid CNN–LSTM model. Unlike RSSI, CSI provides fine-grained subcarrier measurements that capture subtle respiratory dynamics in Non-Line-of-Sight (NLoS) settings; the same granularity has also enabled CSI-based indoor localization in multipath environments, indicating that CSI preserves informative spatial cues beyond conventional RSSI Experimental validation was conducted using low-cost commercial off-the-shelf (COTS) hardware, specifically a Raspberry Pi 4 and a TP-Link router, with signals penetrating a 20 cm brick wall at a 5-meter distance. Our results demonstrate a global detection accuracy of 96% and an Area Under the Curve (AUC) of 0.987 in NLoS scenarios. Comparative analysis shows that the hybrid model significantly surpasses individual 1D-CNN and BiLSTM architectures in classification performance and reliability. The system's efficiency, optimized via TensorFlow Lite for edge computing, ensures low-latency inference while maintaining user privacy. This research underscores the potential of existing Wi-Fi infrastructure for ubiquitous, contact-free medical supervision in complex domestic environments.**

***Index Terms*—Wi-Fi sensing, Channel state information (CSI), Through-wall respiration monitoring, Device-free vital sign detection, CNN–LSTM, Non-line-of-sight (NLoS), Edge deployment, TensorFlow Lite.**

I. Introduction

The growing demand for remote healthcare monitoring, particularly for elderly and chronic patients, has driven the development of non-invasive vital signs detection technologies. Traditional wearable-based approaches present limitations such as user discomfort, battery constraints, and dependence on patient compliance [1]. Consequently, contactless monitoring has emerged as a promising alternative for continuous health assessment in home environments.

Wi-Fi Channel State Information (CSI) has gained attention as a rich source for passive sensing. Unlike Received Signal Strength Indicator (RSSI), which aggregates channel information into a single value, CSI preserves spectral structure at the subcarrier level. This enables detection of subtle body movements associated with respiratory activity and potentially cardiac function [2], [3]. Variations in CSI phase and amplitude encode periodic chest motion, enabling contactless respiratory rate extraction. In addition, breath-status tracking using commodity WiFi CSI supports continuous inference of breathing-related states from temporal signatures [4].

The relevance of this research is evident in scenarios where patients are partially occluded or behind obstacles. In emergency situations or home monitoring of at-risk individuals, contactless solutions using existing Wi-Fi infrastructure enable continuous operation without cameras or permanent instrumentation [5], [6]. Deep learning approaches further improve robustness in heterogeneous environments, enabling reliable respiratory estimation and detection of clinically relevant patterns [7], [8].

The theoretical foundation relies on RF propagation in indoor environments—reflection, scattering, and multipath—where thoracic micromovements modulate the channel and leave measurable traces in CSI amplitude and phase [2], [9]. Time-frequency analysis and phase processing are commonly used to extract respiratory periodicity [3], [10]. However, nonlinear variability in real environments challenges traditional methods. In this context, deep learning models—particularly convolutional neural networks (CNNs) for feature extraction and long short-term memory (LSTM) networks for temporal modeling—learn robust representations directly from CSI time series [11], [12].

The experimental context involves complex indoor environments with obstacles such as walls, doors, and furniture, leading to Non-Line-of-Sight (NLoS) conditions with severe multipath. Therefore, feasibility with common hardware is critical. Commercial routers and platforms such as Raspberry Pi enable practical CSI capture through tools like Nexmon, supporting low-cost and reproducible deployments [13], [14].

The research question guiding this work is: *Is it possible to achieve high accuracy in vital signs detection behind obstacles* *using deep learning models fed by Wi-Fi CSI data?* The hypothesis is that combining CSI preprocessing with CNN–LSTM architectures enables robust respiratory detection under NLoS conditions, contributing to more ubiquitous and privacy-preserving telemedicine systems [15].

Contribution: Unlike prior CSI-based respiration monitoring focused on line-of-sight (LoS) or offline analysis, this work emphasizes: (i) robustness under NLoS conditions with physical obstructions, (ii) deployment on low-cost edge hardware using TensorFlow Lite, and (iii) end-to-end validation using a reproducible pipeline based on commodity Wi-Fi devices. The contribution lies in demonstrating reliable respiration detection under realistic constraints of cost, privacy, and deployment.

Ethics and consent. Data were collected from twelve volunteers under a minimal-risk protocol with informed consent. No personally identifiable information (PII) was recorded; data were pseudonymized, securely stored, and only aggregated results are reported. The study followed applicable ethical guidelines and IEEE ethical conduct principles.

Open Science. DOI: https://doi.org/10.5281/zenodo.19445919

II. Methodology

This section details the system design, including the physical signal model, data acquisition protocol, signal processing pipeline, and the deep learning architecture optimized for edge deployment.

A. Wi-Fi CSI Signal Model

In Orthogonal Frequency Division Multiplexing (OFDM) systems, Channel State Information (CSI) captures the channel response in the frequency domain. The received signal at subcarrier k and time t is modeled as:

$$H_k(t) = |H_k(t)|e^{j\angle H_k(t)} \tag{1}$$

where both magnitude and phase are affected by multipath propagation, reflections, and scattering. The observation per subcarrier can be expressed as:

$$y_k(t) = H_k(t)x_k(t) + n_k(t) \tag{2}$$

where $x_k(t)$ is the transmitted signal and $n_k(t)$ represents additive noise.

These variations encode environmental dynamics and subtle human-induced perturbations, such as thoracic movements caused by respiration. This sensitivity enables CSI to capture fine-grained physiological activity.

To favor operation in the presence of obstacles, the 2.4 GHz band is utilized. This band typically provides better penetration and coverage in indoor environments compared to 5 GHz, increasing the likelihood of capturing meaningful reflected components under Non-Line-of-Sight (NLoS) conditions [2].

TABLE I
EXPERIMENTAL HARDWARE CONFIGURATION

Parameter	Value
Wi-Fi Access Point	TP-Link Archer C50
Receiver	Raspberry Pi 4 Model B
Chipset	Broadcom BCM43455
Frequency	2.4 GHz (Channel 6)
Bandwidth	20 MHz (HT20)
Subcarriers	56 usable
Sampling Rate	50–70 Hz (variable)
Optimizer	Adam
Learning rate	10^{-3}
Loss	Sparse categorical cross-entropy
Batch size	64
Max epochs	60
Early stopping	Patience = 8 (monitor: `val_loss`)
LR schedule	ReduceLROnPlateau (factor = 0.5, patience = 3, min_lr = 10^{-5})
Checkpoint	Best model saved at minimum `val_loss`

B. Experimental Setup and Data Acquisition

1) Hardware Configuration: To ensure reproducibility and practical relevance, we employ low-cost commercial off-the-shelf (COTS) hardware: a Raspberry Pi 4 Model B (Broadcom BCM43455) as receiver and a TP-Link Archer C50 router as transmitter. CSI is extracted using Nexmon CSI on Linux kernel 5.10 [13], consistent with prior CSI sensing deployments on Raspberry Pi-class devices [16].

The RF configuration is summarized in Table I.

2) Scenario and Ground Truth: Two scenarios were evaluated in a standard indoor office environment:

- Line-of-Sight (LoS): 3 m separation
- Non-Line-of-Sight (NLoS): 5 m separation with a 20 cm brick wall fully blocking the direct path

Each acquisition session lasted 120 seconds and was manually annotated as `BREATH` or `AIR`. The `AIR` class corresponds to an empty environment without human presence, ensuring the absence of motion-induced CSI variations.

Acquisition protocol:

- Participants were seated in a fixed position aligned with the transmitter–receiver axis
- Breathing patterns were natural and uncontrolled (no forced rhythm)
- Subjects remained as still as possible to isolate respiratory motion
- Environmental conditions were kept stable during each session

The dataset consists of recordings from twelve volunteers, each contributing multiple sessions per class. However, due to controlled acquisition conditions and the use of a single environment, the overall variability remains limited, which may affect generalization.

C. Signal Processing Pipeline

The data processing pipeline consists of sequential stages designed to improve signal quality and extract relevant respiratory features (Fig. 2).

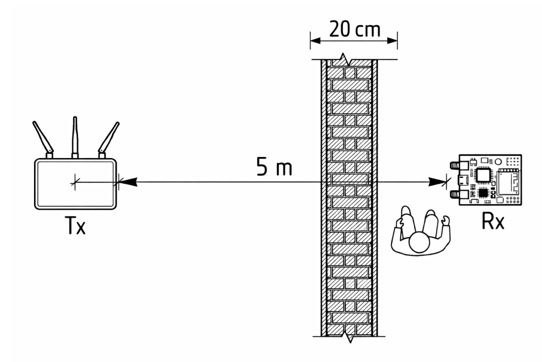

Fig. 1. Schematic diagram of the NLoS experimental scenario. The transmitter (Tx) and receiver (Rx) are separated by 5 m, with a 20 cm brick wall blocking the direct line of sight.

1) **Preprocessing:** CSI-derived feature streams are time-aligned and resampled to a fixed rate. A Hampel filter is applied to suppress impulsive outliers, followed by Z-score normalization to standardize each window [17], [18].
2) **Filtering:** A 4th-order Butterworth bandpass filter (0.1–0.5 Hz) isolates the respiratory frequency band while attenuating low-frequency drift and high-frequency noise.
3) **Segmentation and Normalization:** Signals are resampled to 60 Hz and segmented into fixed-length sliding windows of size T with 50% overlap. Each window is independently normalized using Z-score normalization to improve model stability.

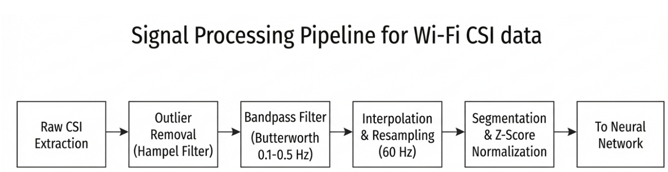

Fig. 2. Flow diagram of the signal processing pipeline. Raw CSI data undergoes filtering, resampling, and normalization before segmentation into fixed-length windows for model input.

D. Deep Learning Architecture

A hybrid CNN–LSTM architecture is employed for supervised respiratory state classification (AIR vs. BREATH) from processed CSI time series (Fig. 3).

- **Input:** a 3D tensor (N, T, F), where N is the batch size, T is the temporal window length, and F is the number of features per timestep. In our implementation, $F = 274$ CSI-derived features.
- **Feature extraction (CNN):** two temporal convolutional blocks:
  – Conv1D (32 filters, kernel size = 7, ReLU) $\rightarrow$ MaxPooling1D(2) $\rightarrow$ Dropout(0.25)
  – Conv1D (64 filters, kernel size = 5, ReLU) $\rightarrow$ MaxPooling1D(2) $\rightarrow$ Dropout(0.25)
- **Temporal modeling (LSTM):** one LSTM layer with 64 units captures temporal dependencies across CSI sequences.
- **Classifier head:** Dense(64, ReLU) with Dropout(0.4)
- **Output:** Dense layer with softmax activation for class probabilities

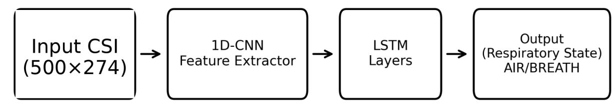

Fig. 3. Block diagram of the proposed CNN–LSTM architecture. Convolutional layers extract local temporal features, while the LSTM captures sequential dependencies.

1) Implementation Protocol: To enable deployment on resource-constrained edge devices, the model was implemented in TensorFlow/Keras and converted to TensorFlow Lite (TFLite) for inference on a Raspberry Pi.

Training was performed using Adam optimizer (lr $= 10^{-3}$) and sparse categorical cross-entropy loss.

To prevent data leakage due to overlapping windows, the train/test split was performed at the **session level prior to segmentation**, ensuring that all windows from a given acquisition session belong exclusively to either training or testing sets.

Dataset composition. Data were acquired separately per class from twelve volunteers, with each session labeled using a single target class.

- Binary setting: `AIR`, `BREATH` (NLoS)
- Multiclass setting: `LOS_AIR`, `LOS_BREATH`, `NLOS_AIR`, `NLOS_BREATH`

We report Accuracy, Macro-F1 score, and ROC-AUC (one-vs-rest for multiclass classification) on the held-out test set.

Remark on evaluation: Due to the limited dataset size and controlled acquisition conditions, this evaluation should be interpreted as a proof-of-concept rather than a fully generalized validation across environments and subjects.

III. Results

The proposed system achieved 96% global accuracy in respiration detection under Non-Line-of-Sight (NLoS) conditions, fulfilling the objective of robust operation behind a 20 cm obstacle. All experiments were executed and evaluated using TensorFlow Lite on edge hardware, demonstrating practical feasibility. The following subsections detail performance analysis and comparisons with baseline architectures.

A. Respiratory State Detection Performance in NLoS

In the binary NLoS scenario (with wall presence), the CNN–LSTM model achieved effective separation between the *NLOS_AIR* and *NLOS_BREATH* classes. As observed in the confusion matrix in Fig. 4, the system correctly classified 52 air instances and 51 breathing instances, with only 1 false negative and 3 false positives.

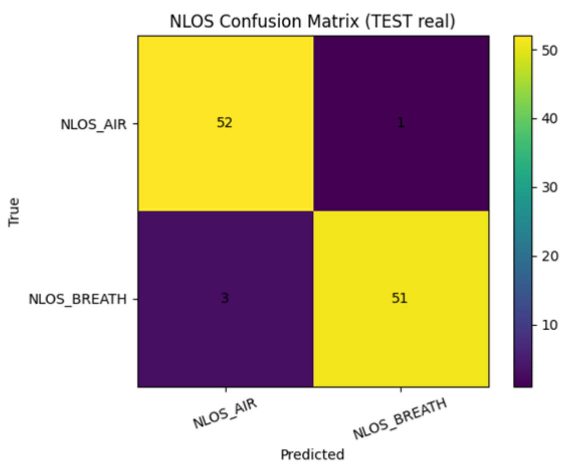

Fig. 4. Confusion matrix for the NLoS scenario (real test set). High diagonal concentration confirms the model's ability to distinguish respiration patterns under obstruction conditions.

Performance metrics on the test set ($N = 107$) include a macro F1-score of 0.96 and an Area Under the Curve (AUC) of 0.987, as shown in Fig. 5. Precision for the *NLOS_BREATH* class reached 0.98, indicating a low false alarm rate, which is critical in practical monitoring scenarios. These results demonstrate robustness against multipath interference, a common limitation in traditional approaches [19].

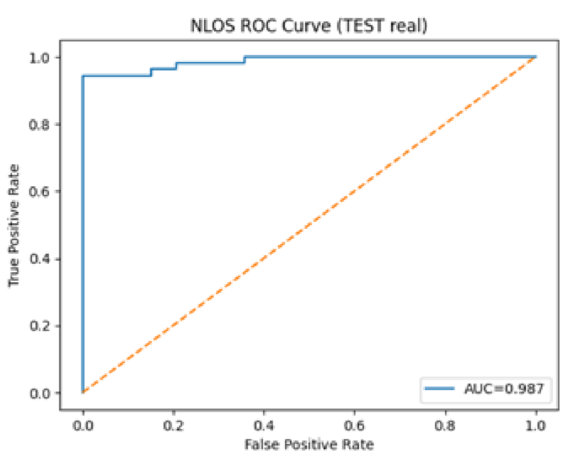

Fig. 5. ROC curve for the CNN–LSTM model in NLoS conditions. The AUC of 0.987 confirms robustness across decision thresholds.

Note: AUC values may differ depending on the evaluation protocol. Fig. 5 reports performance on the held-out test set, while Table II reflects validation performance during model selection. All claims in this paper are based on test-set evaluation.

B. Robustness and Comparative Analysis

To validate the effectiveness of the hybrid architecture, performance was compared against baseline 1D-CNN and BiLSTM models under identical experimental conditions. Table II summarizes the results.

The proposed CNN–LSTM model achieved the highest AUC (0.987), outperforming BiLSTM (0.9633) and 1D-CNN (0.9539). While the 1D-CNN model showed the shortest training time (194.87 s), its classification performance was lower. In contrast, the CNN–LSTM architecture achieves a favorable trade-off between accuracy and computational complexity, making it suitable for edge deployment.

This result is consistent with previous findings that hybrid architectures can better capture both spatial and temporal characteristics of CSI data compared to single-model approaches [20].

TABLE II
PERFORMANCE COMPARISON OF DEEP LEARNING ARCHITECTURES

Model	Params	Time (s)	Test Acc	Test F1	AUC
1D-CNN	76,002	194.87	0.953	0.953	0.954
BiLSTM	280,770	1230.32	0.908	0.906	0.963
CNN-LSTM	**109,026**	**1050.81**	**0.962**	**0.963**	**0.987**

C. Multiclass Scenario and Training Dynamics

In the four-class scenario (LoS/NLoS combined), the global accuracy decreased to 0.68, indicating increased difficulty when distinguishing between environmental conditions and respiratory states simultaneously.

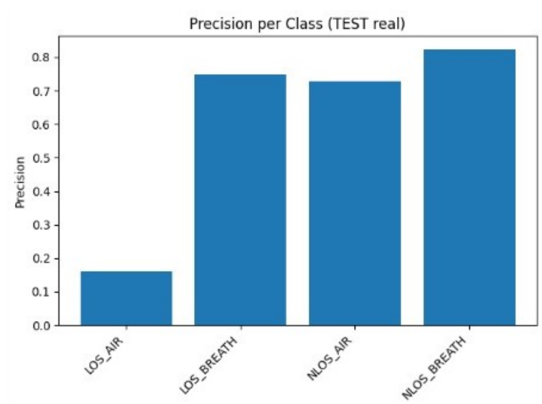

Fig. 6. Precision per class on the real test set for the four-class setting (LOS/NLOS $\times$ AIR/BREATH).

The performance degradation can be attributed to reduced separability between certain classes, particularly *LOS_AIR*. In LoS conditions, the absence of physical obstruction leads to a more stable channel response, where small environmental variations (e.g., hardware noise or multipath fluctuations) may resemble low-amplitude respiratory signals.

This results in overlap in the feature space, making it difficult for the model to distinguish between true absence of motion and subtle physiological activity. Consequently,

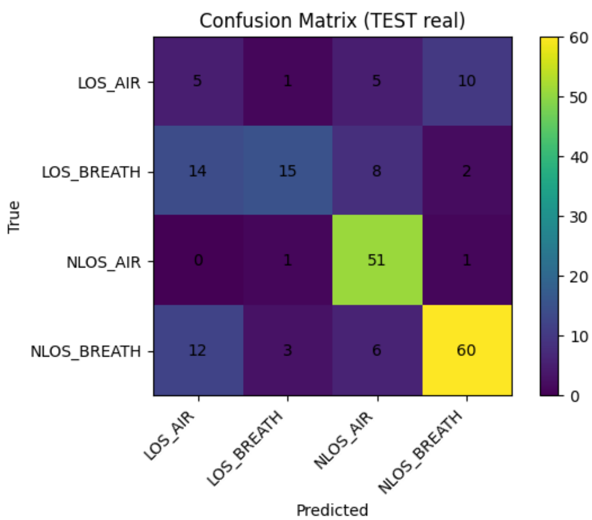

Fig. 7. Confusion matrix for four-class classification. Most errors occur between LoS_AIR and respiration-present classes, highlighting the challenge of distinguishing empty-room LoS conditions from low-amplitude physiological signals.

LOS_AIR shows the lowest precision and contributes most to classification errors.

In contrast, NLoS conditions introduce additional multipath distortions that amplify discriminative patterns in CSI signals. These distortions effectively act as a form of implicit feature enhancement, allowing the model to better distinguish respiration-related variations. As a result, NLoS classes maintain higher precision levels, typically above 0.70–0.80.

These findings suggest that the model is more reliable in detecting the presence of respiration than in confirming its absence under stable channel conditions. This limitation reflects the intrinsic difficulty of modeling “no-signal” states in RF-based sensing systems and has been observed in similar CSI-based studies [21].

D. Edge Computing Efficiency

The CNN–LSTM model was deployed on a Raspberry Pi 4 using TensorFlow Lite, demonstrating real-time inference with low resource usage, supporting practical edge deployment [22], [23].

TABLE III
EDGE DEPLOYMENT BENCHMARK (RASPBERRY PI 4, CPU-ONLY).

Model	Thr	Lat.	P95	RAM
CNN–LSTM	1	41.8	56.2	92.0
CNN–LSTM	4	25.5	35.0	95.0

IV. DISCUSSION

The results support the proposed hypothesis, demonstrating that vital signs can be detected behind obstacles using deep neural networks trained on Wi-Fi CSI data. Achieving 96% accuracy and an AUC of 0.987 under Non-Line-of-Sight (NLoS) conditions confirms robustness in challenging indoor environments with a 20 cm barrier [2].

This performance is partly explained by the 2.4 GHz band, which provides improved indoor penetration [24], facilitating the capture of thoracic micromovements in the RF channel [3].

Compared to prior systems such as PhaseBeat [10], ResFi [25], and UbiBreathe [26], typically evaluated under controlled or line-of-sight conditions, the proposed approach demonstrates reliable performance under NLoS scenarios with strong multipath and attenuation. The CNN–LSTM model (AUC 0.987) outperforms BiLSTM (AUC 0.963), highlighting the advantage of combining spatial feature extraction across subcarriers with temporal modeling [11].

From an application perspective, low-cost hardware such as Raspberry Pi and open-source CSI tools [13] enable scalable, privacy-preserving monitoring without cameras or wearable devices [5], [23], supporting home-based healthcare.

However, limitations remain. The dataset is limited and collected in a single controlled environment, restricting generalizability. The drop to 0.68 accuracy in the multiclass scenario highlights difficulty in distinguishing the *LOS_AIR* class, likely due to spectral similarity between environmental noise and the absence of motion [21]. This suggests that detecting physiological activity is more robust than confirming its absence under stable channel conditions.

Future work includes multi-device cooperative sensing, self-supervised learning for heterogeneous environments [6], and advanced architectures such as attention or residual models [7], [8]. Sensor fusion and additional physiological indicators may further improve robustness [25]. Recent work on location-independent respiration sensing and auxiliary CSI tasks such as presence detection and trajectory recognition [27]–[29] also suggest promising directions for improving generalization.

V. CONCLUSIONS

This work demonstrates the feasibility of non-invasive vital signs detection behind obstacles using Wi-Fi CSI and deep learning. A hybrid CNN–LSTM architecture addresses limitations of wearable-based and line-of-sight monitoring systems [1].

The system achieves 96% accuracy and an AUC of 0.987 under NLoS conditions [24]. The 2.4 GHz band enables penetration of a 20 cm barrier and reliable capture of respiration-induced variations [3], [9]. The CNN–LSTM model outperforms BiLSTM and 1D-CNN by jointly learning spatial and temporal features [11], [12].

Deployment on low-cost edge hardware via TensorFlow Lite enables real-time, privacy-preserving monitoring without cloud dependence [13], [14], supporting practical healthcare applications.

Limitations include reduced performance in multiclass scenarios (accuracy 0.68) due to class overlap, particularly in *LOS_AIR*, and limited dataset diversity [18], [21]. While NLoS conditions enhance discriminative features, improvements are needed for static environments.

Future work will focus on improving generalization through multi-environment data, cross-subject validation, and advanced strategies such as self-supervised and attention-based models [6], [7]. Multimodal sensing and auxiliary CSI tasks may improve robustness without compromising privacy [8], [25]. Extension toward broader activity recognition and SDR-based evaluation pipelines remains a promising direction [30].

ACKNOWLEDGEMENTS

The authors acknowledge the use of the AI system ChatGPT (OpenAI) for language refinement and editing support in specific sections of this manuscript. All technical content, experimental design, and results were developed and validated by the authors.

REFERENCES

[1] Y. Song, W. Taylor, Y. Ge, M. Usman, M. A. Imran, and Q. H. Abbasi, "Evaluation of deep learning models in contactless human motion detection system for next generation healthcare," *Scientific Reports*, vol. 12, no. 1, p. 21592, dec 2022. [Online]. Available: https://www.nature.com/articles/s41598-022-25403-y

[2] Y. Ma, G. Zhou, and S. Wang, "WiFi Sensing with Channel State Information," *ACM Computing Surveys*, vol. 52, no. 3, pp. 1–36, may 2020. [Online]. Available: https://dl.acm.org/doi/10.1145/3310194

[3] D. Zhang, Y. Zeng, F. Zhang, and J. Xiong, "WiFi CSI-based vital signs monitoring," in *Contactless Vital Signs Monitoring*. Elsevier, 2022, pp. 231–255. [Online]. Available: https://linkinghub.elsevier.com/retrieve/pii/B9780128222812000202

[4] D. Zhang, Y. Hu, Y. Chen, and B. Zeng, "BreathTrack: Tracking indoor human breath status via commodity WiFi," *IEEE Internet Things J.*, vol. 6, no. 2, pp. 3899–3911, 2019, doi: 10.1109/JIOT.2019.2893330.

[5] J. C. Soto, I. Galdino, E. Caballero, V. Ferreira, D. Muchaluat-Saade, and C. Albuquerque, "A survey on vital signs monitoring based on Wi-Fi CSI data," *Computer Communications*, vol. 195, pp. 99–110, nov 2022. [Online]. Available: https://linkinghub.elsevier.com/retrieve/pii/S0140366422003127

[6] N. Bao, J. Du, C. Wu, D. Hong, J. Chen, R. Nowak, and Z. Lv, "Wi-Breath: A WiFi-based contactless and real-time respiration monitoring scheme for remote healthcare," *IEEE J. Biomed. Health Inform.*, vol. 27, no. 5, pp. 2276–2285, 2023, doi: 10.1109/JBHI.2022.3186152.

[7] I. Bisio, C. Fallani, C. Garibotto, A. Grattarola, F. Lavagetto, A. Sciarrone, and M. Zerbino, "AI-driven estimation of breathing frequency through CSI analysis," in *Proc. IEEE Int. Conf. Commun. (ICC)*, 2025, pp. 934–939, doi: 10.1109/ICC52391.2025.11161454.

[8] Y. Wang, P. Cheng, S. Li, B. Vucetic, and Y. Li, "High accuracy WiFi sensing for vital sign detection with multi-task contrastive learning," in *Proc. IEEE 99th Veh. Technol. Conf. (VTC-Spring)*, 2024, pp. 1–7, doi: 10.1109/VTC2024-Spring62846.2024.10683244.

[9] S. Yousefi, H. Narui, S. Dayal, S. Ermon, and S. Valaee, "A survey on behavior recognition using WiFi channel state information (CSI)," *IEEE Commun. Mag.*, vol. 55, no. 10, pp. 98–104, 2017, doi: 10.1109/MCOM.2017.1700082.

[10] X. Wang, C. Yang, and S. Mao, "On CSI-Based Vital Sign Monitoring Using Commodity WiFi," *ACM Transactions on Computing for Healthcare*, vol. 1, no. 3, pp. 1–27, jul 2020. [Online]. Available: https://dl.acm.org/doi/10.1145/3377165

[11] E. Shalaby, N. ElShennawy, and A. Sarhan, "Utilizing deep learning models in CSI-based human activity recognition," *Neural Computing and Applications*, vol. 34, no. 8, pp. 5993–6010, apr 2022. [Online]. Available: https://link.springer.com/10.1007/s00521-021-06787-w

[12] D. Khan and I. W. Ho, "Deep learning of CSI for efficient device-free human activity recognition," in *Proc. IEEE 7th World Forum Internet Things (WF-IoT)*, 2021, pp. 19–24, doi: 10.1109/WF-IoT51360.2021.9595661.

[13] M. Schulz, D. Wegemer, and M. Hollick, "The Nexmon firmware analysis and modification framework: Empowering researchers to enhance Wi-Fi devices," *Computer Communications*, vol. 129, pp. 269–285, sep 2018. [Online]. Available: https://linkinghub.elsevier.com/retrieve/pii/S014036641731294X

[14] J. Schäfer, B. R. Barrsiwal, M. Kokhkharova, H. Adil, and J. Liebehenschel, "Human Activity Recognition Using CSI Information with Nexmon," *Applied Sciences*, vol. 1S, no. 19, p. 8860, sep 2021. [Online]. Available: https://www.mdpi.com/2076-3417/11/19/8860

[15] OpenAI, "Chatgpt," https://openai.com/chatgpt, 2026, aI language model used for text editing assistance.

[16] G. Forbes, S. Massie, S. Craw, and C. Clare, "Motion Detection using CSI from Raspberry Pi 4," *arXiv.org*, 2021. [Online]. Available: https://dhalperi.github.io/linux-80211n-csitool/

[17] X. Wang, C. Yang, and S. Mao, "Resilient respiration rate monitoring with realtime bimodal CSI data," *IEEE Sensors J.*, vol. 20, no. 17, pp. 10 187–10 198, 2020, doi: 10.1109/JSEN.2020.2989780.

[18] H. Wang, D. Zhang, J. Ma, Y. Wang, Y. Wang, D. Wu, T. Gu, and B. Xie, "Human respiration detection with commodity wifi devices," in *Proceedings of the 2016 ACM International Joint Conference on Pervasive and Ubiquitous Computing*. New York, NY, USA: ACM, sep 2016, pp. 25–36. [Online]. Available: https://dl.acm.org/doi/10.1145/2971648.2971744

[19] P. Fard Moshiri, R. Shahbazian, M. Nabati, and S. A. Ghorashi, "A CSI-Based Human Activity Recognition Using Deep Learning," *Sensors*, vol. 21, no. 21, p. 7225, oct 2021. [Online]. Available: https://www.mdpi.com/1424-8220/21/21/7225

[20] A. Armenta-Garcia, F. F. Gonzalez-Navarro, J. Caro-Gutierrez, B. L. Flores-Rios, and J. E. Ibarra-Esquer, "BReML: A breathing rate estimator using Wi-Fi channel state information (CSI) and machine learning," in *Proc. Mexican Int. Conf. Comput. Sci. (ENC)*, 2021, pp. 1–8, doi: 10.1109/ENC53357.2021.9534797.

[21] F. S. Abuhoureyah, Y. C. Wong, and A. S. B. Mohd Isira, "WiFi-based human activity recognition through wall using deep learning," *Engineering Applications of Artificial Intelligence*, vol. 127, p. 107171, jan 2024. [Online]. Available: https://linkinghub.elsevier.com/retrieve/pii/S0952197623013556

[22] S. Khan, A. Alzaabi, Z. Iqbal, T. Ratnarajah, and T. Arslan, "A novel digital twin (DT) model based on WiFi CSI, signal processing and machine learning for patient respiration monitoring and decision-support," *IEEE Access*, vol. 11, pp. 103 554–103 568, 2023, doi: 10.1109/ACCESS.2023.3316508.

[23] C. Chen, S. Ohta, T. Nishio, M. Bennis, J. Park, and M. Wahib, "Enabling visual scene recovery from Wi-Fi CSI for occlusion-free surveillance," *IEEE Internet Things J.*, vol. 12, no. 11, pp. 15 040–15 056, 2025, doi: 10.1109/JIOT.2025.3529499.

[24] Y. Wang and J. Sun, "Research on improving accuracy of respiratory sensing based on CSI ratio," in *Proc. 2nd ICCCE*, 2022, pp. 25–28, doi: 10.1109/ICCCE55785.2022.10036209.

[25] J. Hu, J. Yang, J. B. Ong, D. Wang, and L. Xie, "ResFi: WiFi-enabled device-free respiration detection based on deep learning," in *Proc. 17th IEEE ICCA*, 2022, pp. 510–515, doi: 10.1109/ICCA54724.2022.9831898.

[26] H. Abdelnasser, K. A. Harras, and M. Youssef, "UbiBreathe," in *Proc. 16th ACM Int. Symp. Mobile Ad Hoc Netw. Comput. (MobiHoc)*, 2015, pp. 277–286, doi: 10.1145/2746285.2755969.

[27] J. Wan, T. Jiang, X. Zhou, and D. Huang, "Wi-locind: Location-independent respiration sensing based on WiFi CSI," in *Proc. IEEE Wireless Commun. Netw. Conf. (WCNC)*, 2024, pp. 1–6, doi: 10.1109/WCNC57260.2024.10570850.

[28] A. Alteneiji, A. Suliman, K. Poon, and U. Ahmad, "WiFi sensing for presence detection using deep learning," in *Proc. IEEE GCAIoT*, 2024, pp. 1–6, doi: 10.1109/GCAIoT63427.2024.10833586.

[29] Z. Kun, L. Quanquan, and W. Qingzhe, "Harfi: Human trajectory recognition using wifi csi," in *Proc. IEEE Int. Conf. Computer and Communications (ICCC)*, 2023, pp. 1809–1814.

[30] M. Z. Khan, J. Ahmad, W. Boulila, M. Broadbent, S. A. Shah, A. Koubaa, and Q. H. Abbasi, "Contactless human activity recognition using deep learning with flexible and scalable software defined radio," in *Proc. Int. Wireless Commun. Mobile Comput. (IWCMC)*, 2023, pp. 126–131, doi: 10.1109/IWCMC58020.2023.10182652.